Thermal distribution analysis of multi-core photonic crystal fiber laser*

ZHENG Yi-bo(郑一博)[1,2]**, **YAO Jian-quan**(姚建铨)[1], **ZHANG Lei**(张磊)[2], **WANG Yuan**(王远)[1,2], **WEN Wu-qi**(温午麒)[1], **JING Lei**(景磊)[1], **DI Zhi-gang**(邸志刚)[1,3], and **KANG Jian-yi**(康建诩)[1]

1. *Key Laboratory of Optoelectronics Information and Technical Science, Ministry of Education, Institute of Laser & Optoelectronics, College of Precision Instruments and Optoelectronic Engineering, Tianjin University, Tianjin 300072, China*
2. *Hebei Key Laboratory of Optoelectronic Information and Geo-detection Technology, Shijiazhuang University of Economics, Shijiazhuang 050031, China*
3. *College of Information, Hebei United University, Tangshan 063009, China*

(Received 18 August 2011)

The thermal properties of photonic crystal fiber (PCF) laser with 18 circularly distributed cores are investigated by using full-vector finite element method (FEM). The results show that the 18-core PCF has a more effective thermal dispersion construction compared with the single core PCF and 19-core PCF. In addition, the temperature distribution of 18-core PCF laser with different thermal loads is simulated. The results show that the core temperature approaches the fiber drawing value of 1800 K approximately when the thermal load is above 80 W/m which corresponds to the pumping power of 600 W approximately, while the coating temperature approaches the damage value of about 550 K when the thermal load is above 15 W/m which corresponds to the pumping power of 110 W approximately. Therefore the fiber cooling is necessary to achieve power scaling. Compared with other different cooling systems, the copper cooling scheme is found to be an effective method to reduce the thermal effects.

Document code: A **Article ID:** 1673-1905(2012)01-0013-4
DOI 10.1007/s11801-012-1073-8

In recent years, high power rare-earth-doped fiber lasers have attracted considerable attention due to their high effciency and high beam quality compared with the traditional gas and solid-state lasers[1-3]. However, the performance of fiber lasers is limited by mode area and nonlinear effects when they operate at high power. A new class of fiber lasers, called photonic crystal fiber (PCF) lasers, is introduced to overcome the limitations[4-7]. The gain medium of such fiber lasers can be fabricated by doping rare-earth ions into their cores. By surrounding the inner cladding with a web of silica bridges, the double-cladding concept can be transferred to such fibers. The PCF has several attractive properties such as high nonlinearity due to the tight confinement and a shift of zero-dispersion wavelength towards the visible spectral range. Among several PCF lasers, the multi-core photonic crystal fiber (MPCF) laser is particularly interesting, because it can support larger effective mode area, and many theoretical and experimental results have been reported[8-10]. For optical pump lasers, the energy difference between the pump photons and laser photons (called quantum defect) generates a thermal load in the pump region. The temperature in fiber increases with the pump power increasing, which consequently can cause surface damage and coating damage. Though the thermo-mechanical effects could be mitigated due to the distributed nature of the cores, thermal effect still is the dominant limitation factor on power scaling of PCF lasers. Therefore, the analysis of the temperature distribution in MPCF is necessary, which can be used to design the structure parameters of MPCF. There are extensive researches on the thermal effects for double-cladding fiber lasers and photonic crystal fiber lasers reported in the past years[11-17]. In those studies, the air holes in the inner cladding are considered as solid silica, and the influence of the inner air cladding of PCF is neglected.

* This work has been supported by the National Basic Research Program of China (No.2010CB327801), the Key Program of National Natural Science Foundation of China (No.60637010), and the Natural Science Research Project in University of Hebei Province (No.Z2010163).

** E-mail: yibo_zheng@126.com

In this paper, the heat transfer mechanism of high power PCF lasers is studied. The temperature distributions of PCF lasers with a single core, 18 cores and 19 cores are calculated numerically by using full-vector finite element method (FEM). Meanwhile, the temperature distribution of 18-core PCF lasers with different thermal loads is simulated.

In this paper, three PCF configurations with a single core, 18 cores and 19 cores are proposed to fabricate regular PCF lasers, as shown in Fig.1. The cores are ytterbium doped in the structures, and the absorption for the wavelength of 976 nm is as high as 13 dB/m. It offers the possibility to use a short fiber to make the laser cavity. The inner cladding consists of a hexagonal lattice of air holes with the diameter d of 2.2 μm and the hole-to-hole spacing Λ of 10 μm approximately. The air hole in the outer cladding is ellipse, and the major and minor axes are 11 μm and 6 μm, respectively. Each core in the PCF is designed to support a single transverse mode. It can be seen that the radius of the doped core in the single core PCF configuration is about 32 μm as shown in Fig.1(a), and the radius of individual doped-cores is about 7.5 μm in both the MPCF configurations as shown in Fig.1(b) and (c). The total core area in the three PCF constructions is equivalent. The radii of the inner cladding, outer cladding and fiber coating are 126 μm, 223 μm and 300 μm, respectively.

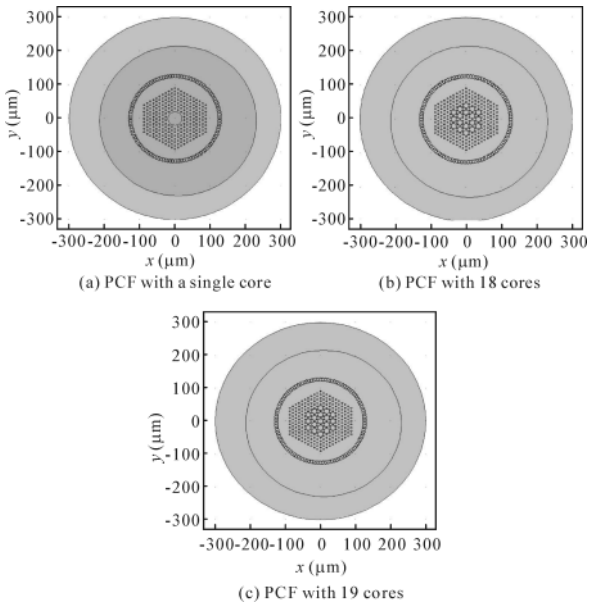

Fig.1 Structures of different PCFs

Heat is mainly generated due to the quantum defect between the pump photons and laser photons in the rare-earth-doped fiber cores. The heat transports from the doped cores to the fiber surface by thermal conduction through fused silica and coating material. In addition, there is convective and radiative heat flow in the chambers of the air-cladding region. Then the heat transports from the fiber surface to the ambient air by thermal convection and radiation. Fig.2 illustrates the heat dissipation model of MPCF. The thermal balance procedure can be divided into the thermal balances inside the fiber and in the surface.

As shown in Fig.2, the thermal load is mainly generated in the doped cores. The heat transfers through the fused silica parts by thermal conduction, and then transfers through the air-cladding region by thermal convection and radiation. For the doped core region, the heat sources concentrate in the cores, so the steady-state thermal conductive equation can be given by[18].

$$\nabla(-k\cdot\nabla T)=Q\ , \tag{1}$$

where k represents the thermal conductivity of material whose value is 1.37 W/(m·K) for fused silica, Q represents the heat power density which can be calculated by $Q=P\alpha\eta/A$, where P represents the pump power, α represents the pump absorption coefficient, η represents the thermal conversion coefficient and A represents the core area. Note that the heat power density here can be defined as a fixed value, because the pump absorption coefficient is varied in different pump lasers.

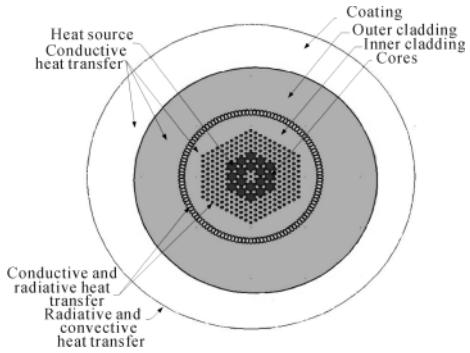

Fig.2 Heat dissipation model of MPCF

For the fused silica region, the heat transfer process can be described as a no heat source conductive equation

$$\nabla(-k\cdot\nabla T)=0\ . \tag{2}$$

For the air chambers region, the conductive heat transfer through the air-cladding region can also be given by Eq.(2), and the radiative heat flow can be given by

$$q=\sigma\varepsilon(T_1^4-T_2^4)\ , \tag{3}$$

where σ=5.6705 × 10^{-8} W/(m^2·K^4) is the Stefan-Boltzmann constant, ε is the emission factor, and T_1 and T_2 are the different temperatures. Note that there is no convective heat transfer in air-cladding region, which is justified by the Grashof number $G_{r\delta}$ in air-cladding region given by[18]

$$G_{r\delta} = \frac{g\alpha\Delta T\delta^3}{\upsilon^2} \quad , \tag{4}$$

where ΔT is the temperature difference between the two sides of air-cladding, and δ is the width of air-cladding. When $G_{r\delta}<$ 2860, there is no convective heat transfer in air-cladding region[18]. In general, the order of δ is 10^{-6}, and the variation range of ΔT is about $0-10^3$ K, so the order of the calculated $G_{r\delta}$ is about $0-10^{-5}$. Therefore, there is no convective transfer in the air-cladding of MPCFs.

In addition, the generated heat is balanced through the convective and radiative heat flow from the outer surface into the ambient air. The convective heat flow is given by

$$q = h(T_{\text{amb}} - T) \, , \tag{5}$$

and the radiative heat flow is given by

$$q = \sigma\varepsilon(T_{\text{amb}}^4 - T^4) \, , \tag{6}$$

where h is the convective coefficient, and T_{amb} is the temperature of the ambient air.

According to the above mechanism analysis, a numerical simulation of temperature distribution across the fiber cross-section can be carried out by using FEM to solve the stationary heat conduction equation, as shown in Fig.3. The values corresponding to different gray-scales represent the temperature. Here we assume that the PCFs are operated with high power which results in a thermal load of 30 W/m approximately, because the thermal load is variable in different experiments. It is seen that the temperature decreases gradually along the radial direction.

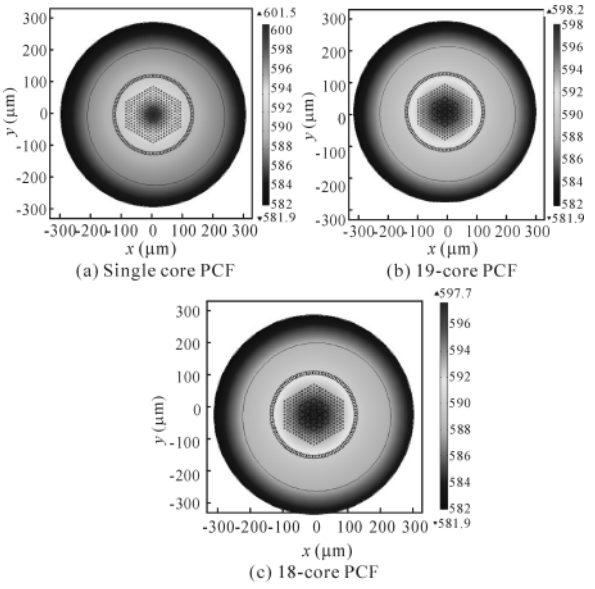

Fig.3 2-D temperature distributions of different PCFs

Fig.4 shows the temperature changes along the radial directions of the three kinds of PCFs. At the fiber center (r=0), the maximum temperatures of the three PCFs are 874.5 K, 871.2 K and 870.7 K, respectively, while the minimum temperature is 854.9 K at surface of the fiber. It can be seen from Fig.4 that the temperature distribution trend is similar, but the curve is uneven, which indicates that both the air hole regions of the inner cladding and outer cladding affect the heat exchange. Moreover, the numerical simulation indicates that the 18-core MPCF is the most effective thermal dispersion configuration.

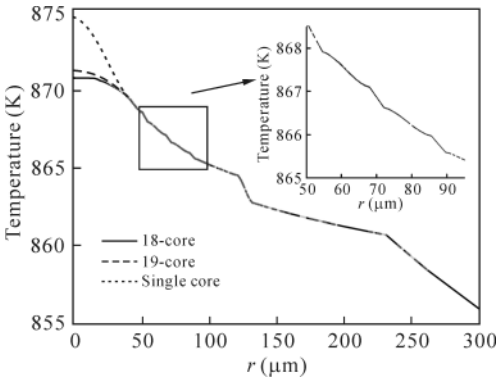

Fig.4 Temperature distributions along the radial direction of different PCFs

The temperature distributions with different thermal loads are illustrated in Fig.5. The calculations reveal that the coating temperature approaches the material critical value of 550 K

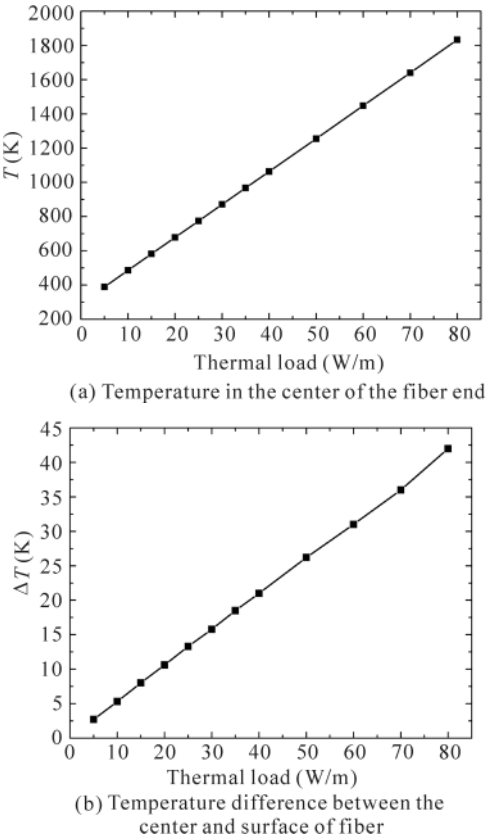

Fig.5 Temperature distributions with different thermal loads

approximately when the thermal load is above 15 W/m, and the temperature of cores approaches the fiber drawing value of 1800 K approximately when the thermal load is above 80 W/m which corresponds to the pump power of about 600 W, as shown in Fig.5(a). It can be seen from Fig.5(b) that the temperature difference increases with the thermal load expanding, and the temperature difference rises up to 42 K when the thermal load is above 80 W/m. So the thermal strain should be considered in high power operation.

According to the analyses above, the temperature must be reduced in high power operation. Therefore the temperature distributions at fiber end with different cooling schemes are simulated as shown in Fig.6. It can be seen that water cooling could be the most valid solution, because the heat transition coefficient of water is two orders of magnitude larger than that of air. For example, the temperature in the center of 18-core PCF is 870.7 K by using air cooling scheme when the thermal load is 30 W/m. If we use water cooling scheme, the center temperature could be reduced to about 479 K and 393 K with the heat transition coefficient of 100 W/(m^2·K) and 200 W/(m^2·K), respectively.

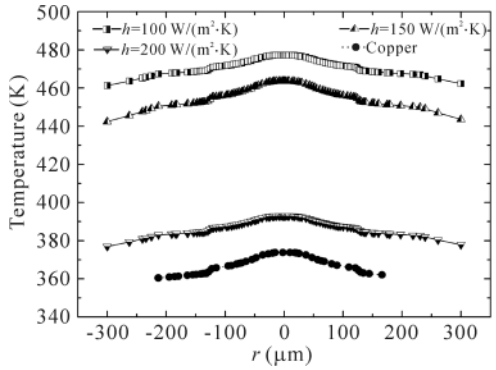

Fig.6 Temperature distribution at fiber end with different cooling conditions

It shows that the main heat dissipation barrier is the fiber surface rather than the air-cladding. However it is difficult to achieve the water cooling equipment in MPCF laser system, so the copper cooling scheme, in which the no-coating MPCF is closely surrounded by a cylindrical copper with the radius of 1 μm, is simulated as shown in Fig.6. The center temperature can be reduced to about 375 K. Therefore, the copper cooling scheme is a better method to reduce the thermal effect.

In summary, we analyze the thermal properties in multi-core PCF laser by using full-vector FEM. Compared with the single core PCF and 19-core PCF, the 18-core PCF is a more effective thermal dispersion construction. The result shows that the temperature distribution along the fiber radial direction is uneven, because both the air hole regions of the inner cladding and outer cladding affect the heat exchange. The air chamber region affects the temperature slightly, and the surface of fibers is the main heat dissipation barrier. The temperatures of inner cladding and core regions could be decreased effectively as increasing the heat transition coefficient of the fiber surface. The temperature distribution of 18-core PCF lasers with different thermal loads is simulated. The results show that the core temperature approaches the fiber drawing value of 1800 K approximately when the thermal load is above 80 W/m. Therefore, the fiber cooling is necessary to achieve high power scaling. Compared with other cooling systems, the copper cooling scheme is found to be an effective method to reduce thermal effects.

References

[1] Y. Yeong, J. K. Sahu, D. N. Payne and J. Nilsson, Opt. Exp. **12**, 6088 (2004).

[2] Ruan Shuang-chen, Yang Bing, Zhu Chun-yan, Lin Hao-jia and Yao Jian-quan, Acta Photonica Sinica **33**, 15 (2004). (in Chinese)

[3] Christopher D. Brooks and Fabio Di Teodoro, Appl. Phys. Lett. **89**, 111 (2006).

[4] J. Limpert, T. Schreiber, S. Nolte, H. Zellmer, T. Tunnermann, R. Iliew, F. Lederer, J. Broeng, G. Vienne, A. Petersson and C. Jakobsen, Opt. Exp. **11**, 818 (2003).

[5] J. Limpert, N. Deguil-Robin, F. Salin, F. Röser, A. Liem, T. Schreiber, S. Nolte, H. Zellmer, A. Tünnermann, J. Broeng, A. Petersson and C. Jakobsen, Opt. Exp. **13**, 1055 (2005).

[6] Jiang Yuanyan, Wei Yangtao, Deng Guoliang, Hu Tao and Feng Guoying, Optoelectronics Letters **6**, 328 (2010).

[7] Chen Wei, Li Shiyu, Wang Dongxiang, Luo Wenyong, Huang Wenjun and Ke Yili, Journal of Optoelectronics • Laser **21**, 1449 (2010). (in Chinese)

[8] Laurent Michaille, David M. Taylor, Charlotte R. Bennett, Terence J. Shepherd and Benjamin G. Ward, Optics Letters **33**, 71 (2008).

[9] Michaille L., Bennett C.R., Taylor D.M. and Shepherd T.J., Selected Topics in Quantum Electronics **15**, 328 (2009).

[10] Xiaohui Fang, Minglie Hu, Chen Xie, Youjian Song, Lu Chai and Chingyue Wang, Optics Letters **36**, 1005 (2011).

[11] Y. Wang, IEEE Photon. Tech. Lett. **16**, 63 (2004).

[12] L. Li, H. Li, T. Qiu, V. L. Temyanko, M. M. Morrell, A. Schülzgen, A. Mafi, J. V. Moloney and N. Peyghambarian, Opt. Exp. **13**, 3420 (2005).

[13] J. Limpert, T. Schreibei, A. Liem, S. Nolte, H. Zellmer, T. Peschel, V. Guyenot and A. Tünnermann, Opt. Exp. **11**, 2982 (2003).

[14] P Elahi, H Nadgaran and F Kalantarifard, Pramana **68**, 529 (2007).

[15] Chen Shuang and Feng Ying, Acta Photonica Sinica **37**, 1134 (2008). (in Chinese)

[16] Han Xiao-ming, Yang De-xing, Zhao Jian-lin, Hou Jian-ping, Duan Kai-liang and Wang Yi-shan, Chinese Journal of Lasers **36**, 2822 (2009). (in Chinese)

[17] Jianfeng Li, Kailiang Duan, Zhiyong Dai, Zhonghua Ou, Yong Liu and Yongzhi Liu, Optik **121**, 1243 (2010).

[18] W. M. Rohsenow, J. P. Hartnett and Y. I. Cho, Handbook of Heat Transfer, New York: McGraw-Hill Companies, 78 (1998).